Chapter 3

Phase transition of finite-sized three-dimensional clusters of charged dust particles in a plasma environment

This chapter contains the work published in "H. Sarma, R. Sarmah, and N. Das, Phys. Rev. E 107, 035206 (2023)".

Molecular dynamics simulation is used to study the dynamics of a harmonically trapped three-dimensional Yukawa ball of charged dust particles embedded in plasma as a function of the external magnetic field strength and Coulomb coupling parameter. It is demonstrated that the dust particles that are harmonically confined arrange themselves into nested spherical shells. When the magnetic field reaches a threshold value at a finite value of the coupling parameter of the dust particle system, the particles begin to rotate in a coherent order. A first-order phase transition from disordered to ordered phase is observed in the magnetically controlled charged dust cluster of finite size. This finite-sized charged dust cluster's vibrational mode freezes at high enough coupling and strong enough magnetic fields, leaving only rotational motion in the system.

3.1 Introduction

It is well known that the dynamics of systems driven far from equilibrium depend on external stimuli. Interesting dynamics may arise in a heterogeneous spatially extended system due to the emergence of collective modes that depend on the nature of instability [124][125][126][127][128][129]. Dusty plasma is an ideal platform to study the physics of both extensive and non-extensive systems (particles interacting via non-collective long-range forces), such as the formation of structures, transitions from ordered to disordered states, stability, etc. The physics of dust clusters may be relevant for the development of microstructures, nano-materials, ions in traps, atomic clusters, etc [130]. Both temporal and spatial scale lengths are stretched in the dusty plasma which can be attributed to the comparatively large size and mass of the dust particles and observation of the phenomena becomes much easier in the laboratory in such a system. Although phase transition is usually studied in the bulk system, it can be still of interest in a finite system, exhibiting novel features and revealing underlying physics. The dust particles immersed in plasma get charged by the flow of plasma ions and electrons or due to radiation in astrophysical systems. The presence of such grains may significantly affect the overall collective behavior of plasma. On the other hand, the plasma particles, specifically the ions mediate the interaction among dust grains and this may often lead to the formation of structures like crystals, clusters, vortices, etc. Whether the system behaves like a collective or non-collective system, depends upon the number of particles present and the geometry of the system. One dimensional string of dust or two-dimensional dust cluster often behaves as a non-extensive system that reflects the properties of ion traps, quantum dots, etc.

The charged dust particles confined in a plasma environment under gravitational and electrostatic forces interact with each other, usually via screened Coulomb (Debye-Hückel) potential. Their behaviors are controlled by the Coulomb coupling parameter (Γ) and the screening constant (κ). A small number of such interacting dust particles under harmonic confinement provided by surrounding plasma may manifest into the formation of a dust cluster. The formation of dust clusters varying from one-dimension to three-dimension in a plasma environment and their structures, and properties in capacitively coupled RF discharge are discussed by

Melzer *et al.* [131]. By suitably controlling the strength of vertical and horizontal confinements, they were successful in producing a 1D dust cluster. A zig-zag transition was also observed when the pressure was controlled externally. Sheridan and Wells [83] determined the critical exponents of such a zig-zag transition. Interestingly, Melzer *et al.* also produced 2-D finite dust clusters where the particles organize themselves into circular shells [103]. They also observed 3-D spherical dust clusters, the so-called Yuakawa ball by suitably controlling the confining forces with a fewer number of ($N = 22$) particles. Depending on the dominant interaction both spherical (in presence of isotropic interaction) and chain-like structures (in presence of attractive wakefield) may be possible. It is to note that the structure of dust clusters embedded in a plasma environment may be significantly influenced by the screening parameter κ (and this introduces a difference to such Yukawa cluster with that of the Coulomb cluster). Baumgartner *et al.* [132] have studied the shell configuration of spherical Yukawa clusters in their ground states for different values of particle number and screening constant. Different properties of the Yukawa cluster such as cluster compression, change of average density profile, a transition from inner to outer shells, etc. were found to be influenced by screening for a given value of particle number. Thus, screening provides a different dimension to the Yukawa dust cluster compared to the Coulomb cluster. The micron-sized dust particles confined in plasma exhibit phase transition similar to solid-to-liquid transition in bulk matter. Nonequilibrium melting of 2-D finite dust cluster caused by instability was investigated by Ivanov *et al.* [91]. They observed a two-step transition from solid to hot crystalline state [90] with a reduction in discharge pressure resulting in unstable oscillations which then transit to fluid state on further reduction of gas pressure. Their results are in good agreement with the nonlinear simulations performed by Schweigert *et al.* [133]. Melting transition in a finite $3-$D cluster, so-called Yukawa balls was experimentally studied by Schella *et al.*[134]. The angular correlation was found to decay before the vanishing of radial correlation. The critical value of the Coulomb coupling parameter was determined for a cluster containing 35 number of dust particles.

The rotation of dust clouds is observed in several experiments of dusty plasma subjected to an external magnetic field. The rotation of particle cloud observed

by Sato *et al.* is attributed to the ion drag force on the fine particles [135][136]. Konopka *et al.* reported that external magnetic field results in a rotation of dust clouds suspended in the sheath of a radio-frequency discharge [137]. They suggested an analytical model that explains qualitatively the mechanism of particle rotation which depends on electrostatic force, ion drag, neutral drag, and effective inter-particle interaction forces. Interestingly, intershell rotation of dust particles in two dimensions was also reported by Maity *et al.* [111] in the absence of a magnetic field which they attributed to the unbalanced electric force between the inner and outer shells.

The study of the behavior of dusty plasma in presence of an external magnetic field may be of profound interest from the point of view of laboratory, fusion plasma, for various industrial applications as well as interstellar, and solar plasma environments. Single dust particle rotation in dc glow discharge plasma in presence of a magnetic field was observed by Karasev *et al.* which they attributed to the impulse exerted in tangential direction by the plasma flux on a particle [138]. Recent experiments on dusty plasma under the influence of an external magnetic field have revealed various interesting properties of such a system. Ordered structures imposed on dusty plasma systems have been observed at high magnetic field strength in magnetized dusty plasma experiment (MDPX) [98]. Dust waves and plasma filamentation have also been observed in the MDPX facility [139]. While a low to moderate-strength magnetic field may influence the dust charging and structure formation via the plasma particle dynamics, a large magnetic field of sufficient strength may have a direct influence on grains which leads to modification in the transport properties of dust through plasma as well as the formation of structures. Dust is an important constituent of the interstellar medium. The coupling of dust with the magnetic field may play a very important role in stellar dynamics [140]. It is known that dust grains grow by accretion and coagulation in dense environments. The study of dust clusters may be of immense importance in such environments. Hirashita [141] has investigated the impact of dust growth on the extinction curve. The purpose of the present study is to investigate the effect of magnetic field and temperature on the dynamical behavior of finite-sized charged dust particles in confined geometry.

3.2 The Model

A three-dimensional dusty plasma containing N dust particles in the background of quasi-neutral plasma confined in a box is considered. The dust grains are assumed to interact among themselves via the repulsive Debye-Hückel potential

$$V(r) = \frac{q_d}{4\pi\epsilon_0 r}\exp(-r/\lambda_d), \tag{3.1}$$

where r is the inter-particle distance between two dust grains, q_d is the dust charge, and λ_d is the dust Debye length. The ion and electron Debye lengths are used to calculate the dust Debye length, which is $\lambda_d = \frac{\lambda_e\lambda_i}{\sqrt{\lambda_e^2+\lambda_i^2}}$, where λ_e and λ_i are the electron and ion Debye lengths, respectively, and are defined as $\lambda_e = \sqrt{\frac{\epsilon_0 k_B T_e}{n_e e^2}}$ and $\lambda_i = \sqrt{\frac{\epsilon_0 k_B T_i}{n_i e^2}}$. In this case, k_B represents the Boltzmann constant, and T_e, n_e and T_i, n_i are the temperature and number density of electron and ion respectively. The isotropic harmonic potential is taken into consideration as a confinement model [85, 86]. The superposition of the ion drag force, electric field, thermophoretic, and gravitational forces acting on the dust particles is assumed to be represented by the harmonic potential.

$$H = \frac{1}{2m}\sum_{i=1}^{N}(\mathbf{p_i} - q_d\mathbf{A}_i)^2 + q_d\phi, \tag{3.2}$$

where,

$$q_d\phi = \frac{q_d^2}{4\pi\epsilon_0}\sum_{i=1}^{N-1}\sum_{j=i+1}^{N}\frac{\exp(-r_{ij}/\lambda_d)}{r_{ij}} + \frac{1}{2}m\omega^2\sum_{i=1}^{N}r_i^2. \tag{3.3}$$

Here, r_i is the distance of the i^{th} particle from the center of the box and $r_{ij} = |\mathbf{r_i} - \mathbf{r_j}|$. m and q_d are mass and charge of a dust particle respectively and λ_d is Debye length of the dust grains. ω denotes the strength of the confinement potential. The equation of motion of the i^{th} particle is

$$m\ddot{\mathbf{r}}_i = q_d(\mathbf{v}_i \times \mathbf{B}) - q_d\nabla\sum_{j\neq i}^{N}V(r_{ij}) - m\omega^2\mathbf{r}_i, \tag{3.4}$$

where $V(r_{ij})$ is the Debye-Hückel potential operating among the dust grains, $q_d(\mathbf{v_i} \times \mathbf{B})$ is the Lorentz force experienced by the charged dust particle as a result of the magnetic field, and the final term is the confining harmonic force. Using the following scaled variables, we further recast Eq. 4.3 into dimensionless form, $\mathbf{r'} = \mathbf{r}/\lambda_d$, $\tau = \sqrt{\frac{k_B T_d}{m\lambda_d^2}}t$, $\mathbf{B'} = \frac{q_d\lambda_d}{\sqrt{mk_B T_d}}\mathbf{B}$ and $\Omega^2 = \frac{m\lambda_d^2}{k_B T_d}\omega^2$ respectively. Next,

using scaled variables, the dimensionless equation of motion is as follows:

$$\ddot{\mathbf{r}}'_i = (\mathbf{v}'_i \times \mathbf{B}') + \Gamma\kappa \sum_{j\neq i}^{N} \frac{\left[1 + r'_{ij}\right]}{{r'_{ij}}^3} \exp\Big(-r'_{ij}\Big)\mathbf{r'_{ij}} - \Omega^2 \mathbf{r'_i}. \tag{3.5}$$

The overdot now refers to the redefined time derivative. Γ and κ are the Coulomb coupling and screening parameters, respectively, and T_d is the dust kinetic temperature. These are specified as follows:

$$\Gamma = \frac{q_d^2}{4\pi\epsilon_0 r_{av} k_B T_d}, \tag{3.6}$$

and

$$\kappa = \frac{r_{av}}{\lambda_d}. \tag{3.7}$$

Here, n_d is the dust particle's number density, and r_{av} is the average inter-particle distance of the charged dust particles, which is defined as $r_{av} = (\frac{3}{4\pi n_d})^{1/3}$. $\Gamma > 1$ denotes a strongly coupled state, where the average interparticle interaction energy is greater than the average thermal energy, while $\Gamma < 1$ denotes a weakly coupled state[53]. The effect of temperature in the dynamics of the Yukawa cluster enters via the Coulomb coupling parameter.

3.3 Simulation scheme

Molecular dynamics simulation has been performed on a 32 number of charged dust particles placed inside a cubical simulation box interacting via Debye-Hückel potential (see Eq. 3.1). The size of the simulation box is chosen as $L_x = L_y = L_z = 6.83 \times 10^{-4}$m. A modified version of the velocity-verlet algorithm has been used to integrate the equations of motion [107]. In the simulation, the values of ion, electron, and dust number densities respectively are $n_i = 10^{15}\ m^{-3}$, $n_e = 8.89 \times 10^{14}\ m^{-3}$ and $n_d = 10^{11}\ m^{-3}$ and the electron and ion temperatures respectively are $T_e = 2320\ K$ and $T_i = 2050\ K$ [142]. The mass of the dust particles is taken to be $m = 6.99 \times 10^{-13}\ kg$ [85, 111]. The value of the screening parameter is calculated and is kept fixed at $\kappa = 1.8$ for all the runs. The frequency of the harmonic potential is fixed at $\omega = 50\ Hz$.

A simulation run starts from a random initial configuration of the particles. For each run, the number of particles, volume, and temperature are kept fixed. To

simulate at a fixed temperature, Berendsen thermostat [143, 144] has been used. Data is gathered for the subsequent 1.0×10^5 steps after the system is connected to the Berendsen thermostat for the first 1.4×10^6 steps to bring the system to equilibrium at the target temperature.

3.4 Results and Discussion

Studying the dynamics and phase transition of the Yukawa dust cluster in the presence of an external magnetic field is the main goal of the current work. $N = 32$ point-sized charged dust particles are used in the simulation. The coupling parameter Γ, the applied magnetic field B, the screening constant $\kappa = r_{av}/\lambda_d$, and the frequency of the harmonic potential ω are the physically relevant parameters in our model. We fixed the frequency $\omega = 50\ Hz$ and the screening constant $\kappa = 1.8$ in order to lower the number of free parameters. The applied magnetic field B regulates the effective dynamics, whereas the kinetic energy of the charged dust particles is determined by temperature or the Coulomb coupling constant Γ. The typical parameters Γ and B are adjusted for a wide range of values in order to comprehend the dynamics of the dust particle system with the coupling strength and the applied magnetic field. The magnetic field B is adjusted for the current inquiry between 0.001 and 0.7 T. In contrast, the dust temperature is adjusted between 293 and 40000 K to change the coupling parameter Γ. Several dusty plasma experiments have shown abnormally high dust kinetic temperatures [145][146][147]. The interplay between repulsive Debye Hückel and the confining harmonic potential results in the shell-like arrangement of the cluster of dust particles. For the parameters used here, charged dust particles organize themselves into two nested shells with a configuration (5, 27). This configuration remains invariant under any change in the magnetic field. Figure 3.1(a) shows a snapshot of the dust particle cluster and Fig. 3.1(b) depicts the time evolution of the particle trajectories for $\Gamma = 514.38$ at zero magnetic fields. The organization of the particles into two shells can be seen in Fig. 3.1(c) which shows the radial position of the particles measured from the center of the simulation box.

3.4.1 Dynamics of the charged particles as a function of magnetic field and Coulomb coupling parameter

To understand the equilibrium properties of the charged dust particles as a function of the magnetic field, the Columb coupling constant is fixed and the dynamics of the particles as a function of the applied magnetic field B have been studied. The particle trajectories for different values of magnetic field B are shown in Fig. 3.2. The charged dust particles exhibit interesting dynamics as a function of the magnetic field with the fact that the particles are organized into two distinct shells as shown in Fig. 3.1(a). Since the dust particles are charged particles and the magnetic field is applied along the $z-$direction, the dust particles will experience a Lorentz force and start rotating about the $z-$axis. However, contrary to it, at

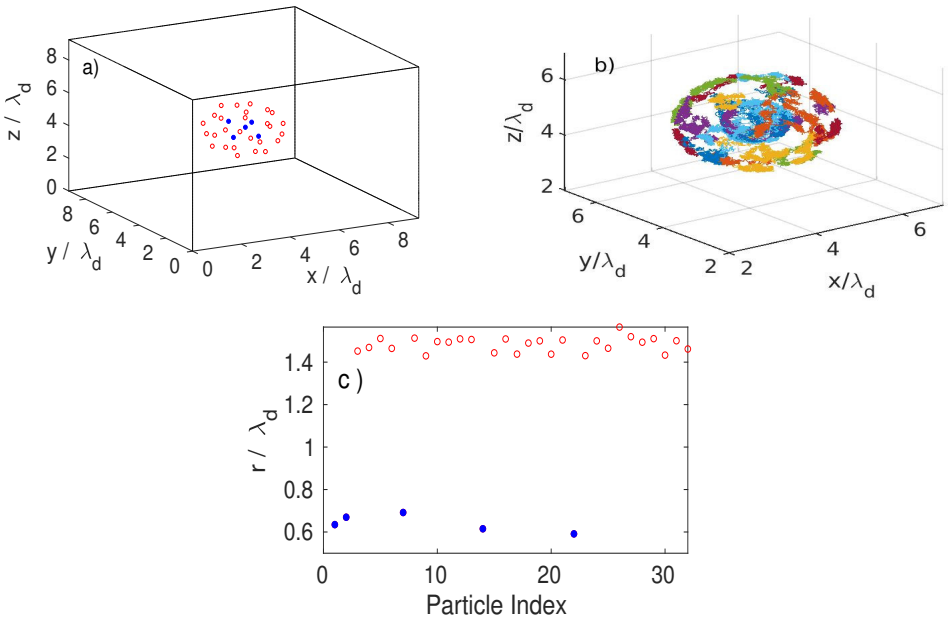

Figure 3.1: Configuration of the dust particles in the cluster containing $N = 32$ particles at $\Gamma = 514.38$ and $B = 0\ T$. (a) A snapshot of the shell configuration of the dust cluster. The filled circles represent particles on the inner shell, and the open circles represent the outer shell particles. (b) The trajectories of the particles for 1.0×10^5 timesteps. (c) The radial position of the particles measured from the center of the simulation box at the final timestep of the simulation.

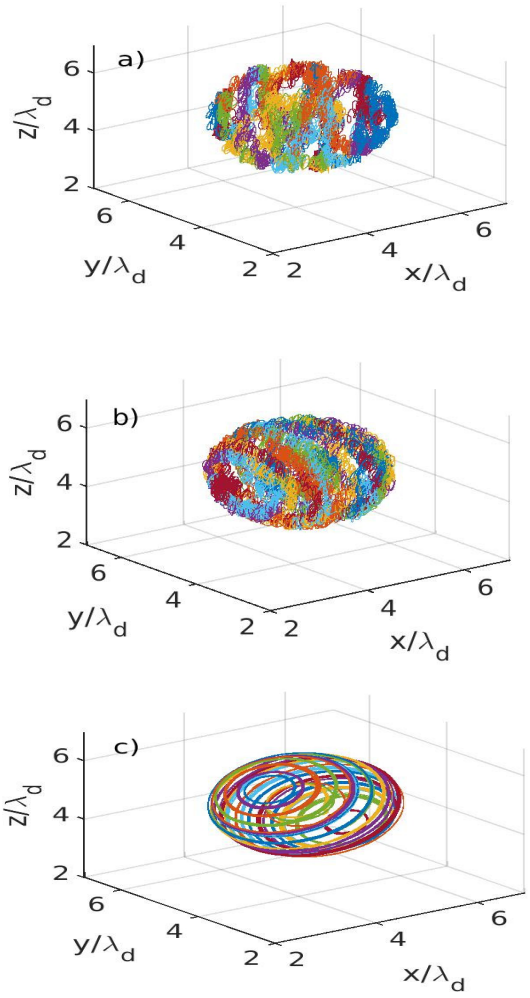

Figure 3.2: Dust particles' trajectories for three different values of the applied magnetic field strengths (a) $B = 0.001\ T$, (b) $B = 0.4$ T, and (c) $B = 0.6$ T, for $\Gamma = 21.11$.

a low applied magnetic field $B = 0.001\ T$, the mean trajectories of the charged dust particles show rotation about a random orientation. Considerable fluctuation about the mean trajectory is evident in Fig. 3.2(a). The trajectory plot suggests that the charged dust particles attain vibrational motion along with rotational motion. The rotational motion is due to the external magnetic field, and the vibrational motion about the mean can be attributed to the thermal energy. As the magnetic field increases, at $B = 0.4\ T$, the system of particles tries to attain a definite axis of rotation. However, the fluctuation in the mean trajectory of a particle attributed to vibrational mode due to thermal energy remains. Further

increase of the magnetic field to $B = 0.6\ T$, a drastic change in the dynamics of the system of particles is observed. In this magnetic field strength, the vibrational motion of the trajectories around the mean trajectories of the system of particles completely ceases to retain only the rotational motion. Thus, the charged dust particles show a phase transition from disordered rotation to ordered rotational motion. The system of dust particles has collectively developed a phase where all the particles rotate about a distinct axis.

The fact that the collective dynamics of the dust particles at a given coupling parameter change drastically as a function of the applied magnetic field induce us to explore the possibility of the effect of coupling strength. Thus, the coupling

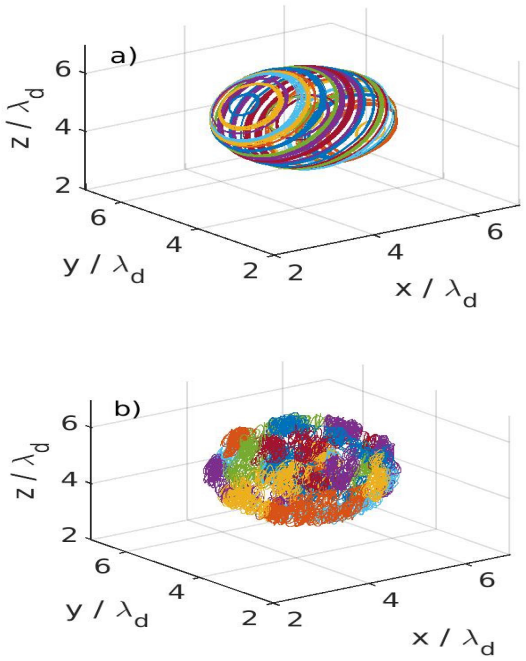

Figure 3.3: Dust particles' trajectories at two different coupling strengths (a) $\Gamma = 15.43$, (b) $\Gamma = 12.86$ keeping magnetic field fixed at $B = 0.6$ T.

parameter is varied keeping the magnetic field fixed. The representative trajectory for two different values of coupling parameter keeping the magnetic field fixed at $B = 0.6\ T$ is shown in Fig. 3.3(a,b). It is observed that at low coupling strength for a fixed magnetic field, the dust particles have both rotational as well as vibrational modes. The dust particles acquire vibrational motion about the mean trajectory along with the rotational motion. At high coupling strength values,

however, the vibrational symmetry breaks and the charged dust particles rotate uniformly about a fixed axis, suggesting a phase transition from the high symmetry phase to the low symmetry phase. Competing length and time scales in the system rationalize the dust particle's shift in behavior. By reducing the average interparticle distance between the charged dust particles, the force resulting from the repulsive Debye Hückel potential balances with the attractive harmonic force in equilibrium for high values of the Coulomb coupling parameter and strong magnetic fields. The magnetic field subsequently transforms the whole kinetic energy into rotational energy. The particle system thus achieves a fixed axis of rotation. The particle trajectories are limited within these two equilibrium energy shells at smaller values of the Coulomb coupling parameter, where the equilibrium repulsive potential intersects the harmonic potential at two places. All of the kinetic energy cannot be transformed into rotational energy by the weak magnetic field. As a result, the particle system continuously alternates between these two equilibrium energy shells, which are the source of the particles' vibrational mode. A phase transition as a function of the control parameters, namely the coupling parameter Γ and magnetic field B, is suggested by the aforementioned analysis of the particle trajectories.

3.4.2 Phase transition

Phase transition represents singularities in free energy functional as the control parameter of the system is varied. In a macroscopic system Lindemann parameter, defined as particle position fluctuation normalized by interparticle distance or relative interparticle distance fluctuation (IDF) shows a sudden jump during the melting. The IDF is defined mathematically as [134],

$$u_{rel} = \frac{2}{N(N-1)} \sum_{i=1}^{N-1} \sum_{j=i+1}^{N} \sqrt{\frac{< r_{ij}^2 > - < r_{ij} >^2}{< r_{ij} >^2}}. \tag{3.8}$$

In a finite system, it is challenging to see the discontinuous shift in the IDF that characterizes a phase transition. We use the method proposed by Boning *et al.* [109] to detect order-disorder transition in finite-size systems because the number of particles in our system is restricted to ($N = 32$) tiny numbers. One possible diagnostic method for locating transition points is the variance of block-averaged inter-particle distance fluctuation (VIDF). The order parameter of macroscopic

systems in finite-size systems can also be represented by the VIDF. It is computed by first splitting the equilibrium simulation length into a fixed number of blocks (M) with equal durations, then figuring out the IDF u_{rel} for each block. The VIDF is then described as,

$$\sigma =< u_{rel}^2 > - < u_{rel} >^2, \tag{3.9}$$

where,

$$\begin{aligned} < u_{rel}^2 > &= \frac{1}{M}\sum_{\alpha=1}^{M} u_{rel}^2(\alpha), \\ < u_{rel} > &= \frac{1}{M}\sum_{\alpha=1}^{M} u_{rel}(\alpha). \end{aligned}$$

In a finite-size system, Boning *et al.* showed that the VIDF shows a clear peak during the melting transition. As a result, transition point identification is highly effective. One parameter is held constant while the other is changed in order to determine the critical values of the coupling constant and the magnetic field. Initially, the VIDF is computed across a broad range of magnetic fields with the Coulomb coupling value Γ fixed. The VIDF with a change in the magnetic field

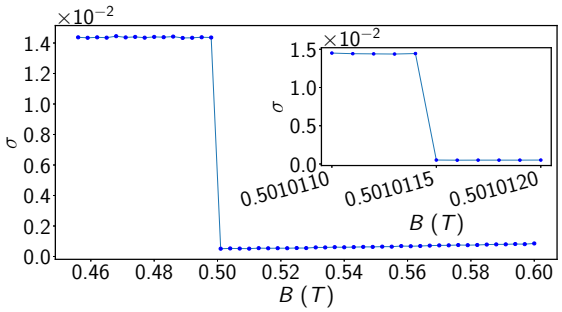

Figure 3.4: Variation of the variance of block averaged inter-particle distance fluctuation (σ) to the strength of the magnetic field B for fixed $\Gamma = 21.107216$.

strength for $\Gamma = 21.107216$ is displayed in Fig. 3.4. The magnetic field is scanned more closely in the inset. A singularity is indicated by the abrupt discontinuity in the VIDF at around $B \sim 0.5\ T$. By breaking the vibrational symmetry of low magnetic field strength, the system of particles experiences a phase transition from a disordered rotation to an ordered rotating phase, as revealed by the investigation of the charged dust particle trajectories. The critical magnetic field value for this

transition is $B_c = 0.5010114\ T$ at $\Gamma = 21.107216$, as even a small increase in field strength causes VIDF to drop sharply to a lower value.

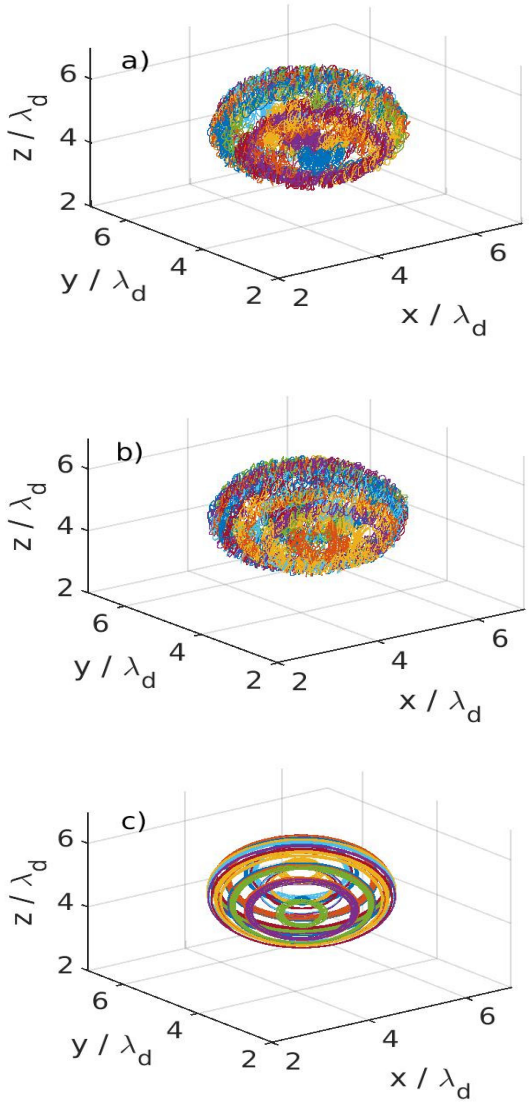

Figure 3.5: Plot of trajectories of the dust particles at the critical magnetic field strength $B_c = 0.5010114\ T$, for three different coupling strengths (a) $\Gamma = 21.107211$, (b) $\Gamma_c = 21.107216$, and (c) $\Gamma = 21.107219$

The influence of coupling strength around this critical magnetic field is also examined to determine whether the transition of the dynamics of the system of the finite number of dust particles is real. The coupling strength of the dust particles can be changed by maintaining the magnetic field's magnitude at $B_c = 0.5010114T$. As the coupling strength deviates significantly from the critical

value $\Gamma_c = 21.107216$ (Fig. 3.5), the dynamics of the particle system undergoes an abrupt change. The dynamics remain unchanged when the dust particles' coupling strength is increased further. The system of dust particles exhibits unique collective dynamics at the critical point (B_c, Γ_c), as this study illustrates. Beyond the critical point, the system's behaviour substantially changes, indicating the creation of two distinct phases surrounding the critical points. This exercise implies that at the critical point (B_c, Γ_c), the system experiences a first-order phase transition. The VIDF as a function of the coupling strength Γ is plotted at the critical magnetic field $B_c = 0.5010114\ T$, as illustrated in Fig. 3.6, to determine if the transition is caught by the VIDF (σ). The discrete drop at the critical

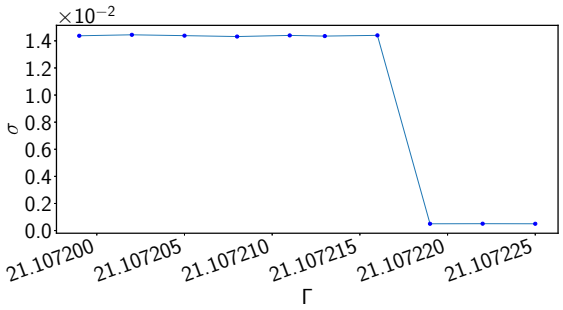

Figure 3.6: Variation of the VIDF with coupling parameter at the critical magnetic field 0.5010114 T.

value of the coupling strength $\Gamma_c = 21.107216$, clearly indicates that the system undergoes a first-order phase transition at this critical point. Further increase in the coupling parameter does not induce any change in the VIDF suggesting that the system behaves collectively above the critical point. Using the VIDF as the signature of this first order ordered to the disordered rotational phase, the phase diagram in the $B - T$ plane (since $\Gamma \propto 1/T_d$) separating the two phases is shown in Fig. 3.7. The critical magnetic field (B_c) corresponding to a dust temperature (T_c) or coupling strength (Γ_c) show a power law dependency $B_c = AT_c^{\alpha}$ at the fixed dust density n_d with exponent $\alpha = 0.5$ and $A = 5.8 \times 10^{-3}\ TK^{-1/2}$. Thus, the phase boundary separating the two phases at a fixed dust density and finite dust temperature follows the equation of state,

$$\frac{B_c}{\sqrt{T_c}} = Const. \tag{3.10}$$

The emergence of the square root dependence of the critical magnetic field on the

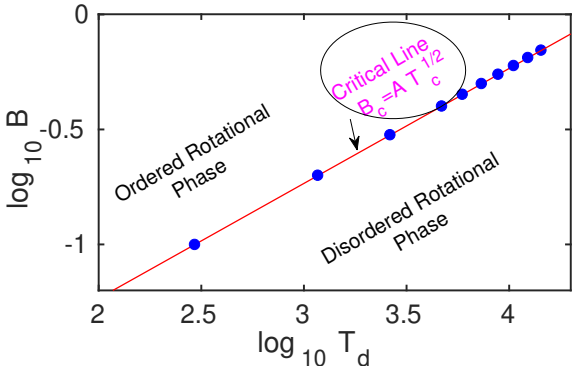

Figure 3.7: The $B-T$ phase diagram separating ordered-to-disordered rotational phase of the finite-sized system of dust particles. The circles indicate numerically obtained data points and the straight line is the critical line satisfying the equation of state $B_c = A\sqrt{T_c}$ with $A = 5.8 \times 10^{-3}\, TK^{-1/2}$.

dust temperature is easy to understand from the following physical picture. The order-to-disorder transition is characterized by the onset of coherent rotation about an axis when the magnetic field is applied. The overlapping of the trajectories of the particles in the disordered state disappears and the particles rotate in distinct well-defined trajectories. The kinetic energy due to the available thermal energy of the dust particles is then completely converted into rotational energy by the magnetic field. For coherent rotation in thermal equilibrium, each charged dust particle rotates about the fixed axis of rotation with an angular velocity $\dot{\theta}$. Then, the available thermal kinetic energy $\sim k_B T_c$ equals the rotational energy $I\dot{\theta}^2/2$ of the dust particle which may be the superposition of rotational energy of cyclotron motion with angular velocity $\frac{q_d B_c}{m}$ and a rotational drift suggesting $B_c \propto \sqrt{T_c}$. Below the critical magnetic field B_c, for a fixed dust temperature T_d, the available thermal energy decomposes into rotational and linear kinetic energy. The excess linear kinetic energy then give rise to the vibrational motion around the mean giving rise to disordered rotational phase.

3.4.3 Structure dynamics of dust particles

To study the structural properties of the dust clusters, the radial distribution function has been used. The radial distribution function (RDF) is proportional to

the probability of finding a pair of particles separated by a distance in the range r to $r + dr$ from a reference particle and is defined as[108],

$$g(r) = \frac{1}{N}\Big\langle \sum_{i}^{N} \sum_{j \neq i}^{N} \delta(r - r_{ij}) \Big\rangle. \tag{3.11}$$

It gives an idea of how the particles arrange themselves around one another.

To get an insight into the structure of the dust cluster with coupling strength Γ, RDF has been calculated for a range of the Coulomb coupling parameter Γ, initially for a magnetic field $B = 0\ T$. An analysis similar to the previous section suggests that at $\Gamma_c = 314.67$ a transition from a disordered state to an ordered state takes place. This can also be seen from the plot of $g(r)$. The plot

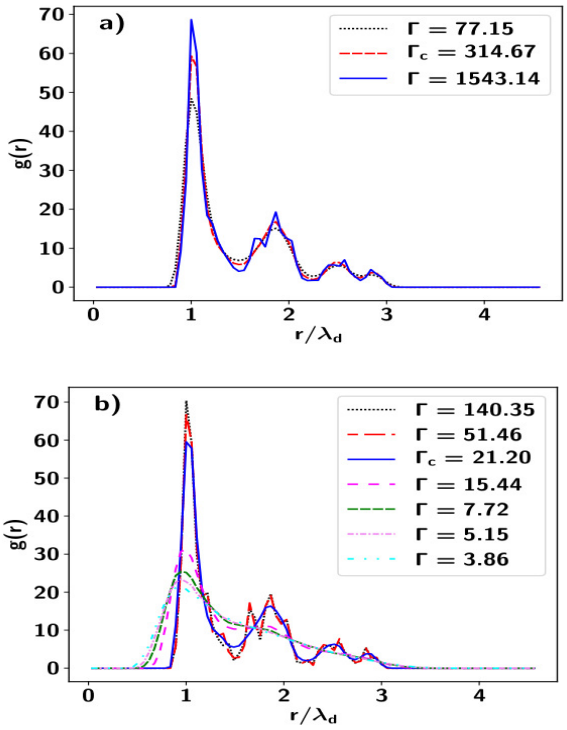

Figure 3.8: The radial distribution function $g(r)$ with Γ at (a) $B = 0\ T$ (b) $B = 0.5\ T$.

of the RDF for different values of Γ at a magnetic field $B = 0\ T$ is shown in Fig. 3.8(a). For $\Gamma = 77.15$, the RDF suggests a liquid-like structure. However, the height of the first peak of $g(r)$ is seen to increase with increasing value of coupling parameter Γ from 77.15 to 1543.14 and there is partial development of secondary peaks beyond $\Gamma_c = 314.67$ suggesting correlation like partially crystallized state.

On the other hand, at $B = 0.5$ T of Fig. 3.8(b), the height of the first peak initially increases gradually from 3.86 to 15.44 and then exhibits a sudden change corresponding to $\Gamma = 21.20$. The sharp peaks of $g(r)$ beyond the $\Gamma = 21.20$, suggest a strong correlation among the particles at large distance reminiscent of the fixed position of particles like solid. Furthermore, for the value of $\Gamma = 51.46$ and $\Gamma = 140.35$, the RDF almost superimpose each other which suggests the structure of the dust particles remains invariant with the change. The sudden change in the peak height and development of subsequent peaks of $g(r)$ is a signature of the transition from a disordered to an ordered state.

As shown in Fig. 3.5 the trajectories are very sensitive to the change in the values of the Coupling strength which indicates the fact that the static structure of the cluster is also sensitive to the change in coupling strength. This is proven by the RDF plots shown in Fig. 3.9.

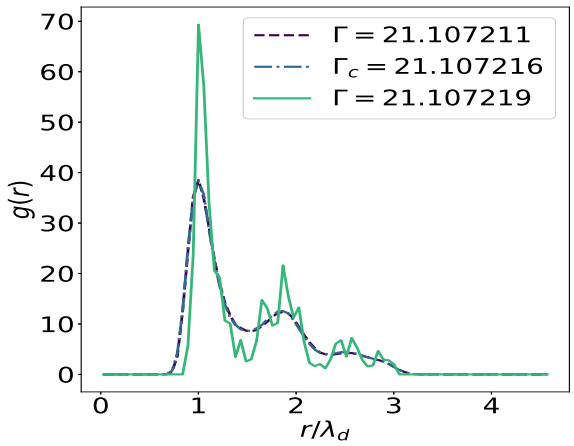

Figure 3.9: The Radial Distribution Function at three different values of Γ around the transition point at $B = 0.5010114\,T$ at $\kappa = 1.8$.

3.5 Conclusions

In conclusion, the dynamics of a finite-sized cluster of charged dust under an external magnetic field, a confining harmonic, and a repulsive Debye-H"uckel potential have been examined. The charged dust particles form two nested spherical shells with no long-range order, resembling a fluid-like condition, when the sup-

plied magnetic field is absent at a limited value of coupling strength. Similar to particles in their gaseous forms, the dust particles randomly organise at very low coupling strengths. The dust particles move randomly about the surface of the two nested spheres without a clear axis of rotation as soon as the magnetic field is activated, at a weak magnetic field and small coupling parameter (or high temperature). Both rotational and vibrational motions are present in the particles in this state. The particles are arranged randomly on the sphere, as shown by the radial distribution function in this stage. The dust particles rotate in order around a specific axis of rotation when a collective mode appears at a high magnetic field for a particular coupling strength. When a low magnetic field's vibrational symmetry is broken, this collective mode appears. Curiously, with a fixed magnetic field, the collective mode can also be obtained by adjusting the temperature of the dust particles or the coupling parameter. At a constant dust density and finite temperature, this provides us with a phase boundary between the orientationally ordered rotating fluid and disordered rotating fluid phase that satisfies an equation of state $B_c/\sqrt{T_c} = Const.$ The available thermal energy transformed into rotational energy by the applied magnetic field causes the square root dependence of the critical magnetic field on the dust temperature. Because of the dynamical equilibrium between the attractive and repulsive potentials, our study demonstrates that the system of dust particles naturally arranges itself in spherical shells regardless of the magnetic field's strength. Determining the dynamics of stars' magnetic fields during their early development could be aided by this research. It is still unknown, though, what microscopic mechanism causes dust clusters to rotate when exposed to a magnetic field. The ion drag model is used to explain the observed rotation in the majority of the experiments[137][135][148]. Conversely, in their experiment of a dust cluster in an inductively coupled rf plasma with an external magnetic field, Cheung *et al.* had noted that the estimated value of ion drag force needed for the observed rotation was significantly lower and that it could not be held entirely responsible for the rotational motion[149]. We ignore the effects of dust-neutral collision and ion dynamics in favour of concentrating on the dust dynamics in the presence of the external magnetic field's Lorentz force, confining potential, and repulsive inter-particle Yukawa interaction. Interestingly, once the magnetic field surpasses a threshold value, the dust cluster shows coherent rota-

tion even without ion dynamics and associated $\mathbf{E} \times \mathbf{B}$ drift. The connection of the Lorentz force with the Yukawa and harmonic force residue may be the source of this rotating motion. A more thorough investigation is now being conducted and will be necessary to fully comprehend this process.